for the Halley nucleus.
18. Hyakutake nucleus diameter estimates based on infrared observations are 4.2 ± 0.8 km [J. Sarmecanic, M. Fomenkova, B. Jones, T. Lavezzi, *Astrophys. J.* **483**, L69 (1997)] and 4.8 ± 1.0 km [Y. R. Fernandez *et al.*, *Bull. Am. Astron. Soc.* **28**, 1088 (1996)]. The infrared diameters, if correct, lower the radar albedo to 0.012, implying a surface with the consistency of loosely packed snow. Diameter upper limits based on radio continuum measurements are 5.0 km [I. de Pater *et al.*, *Planet. Space Sci.* **45**, 731 (1997); W. J. Altenhoff *et al.*, *Bull. Am. Astron. Soc.* **28**, 928 (1996)], 6.0 km [Y. R. Fernandez, A. Kundu, C. M. Lisse, M. F. A'Hearn, *Planet. Space Sci.* **45**, 735 (1997)], and 5.7 km (*28*).
19. D. K. Yeomans, personal communication.
20. The standard model of grain ejection by gas drag (*5*) gives a terminal grain velocity $V = Ca^{-1/2}g$. The gravity correction $g = (1 - a/a_m)^{1/2}$ is a function of the maximum liftable grain radius $a_m = 9V_g/\dot{\mu}/16\pi R\rho_n\rho G$, where V_g and $\dot{\mu}$ are the gas velocity and gas mass flux at the surface, R is nucleus radius, ρ_n and ρ are the nucleus and grain densities, and G is the gravitational constant.
21. A survey of all ejection directions shows a locus of directions giving fits with χ^2_ν better than 1.08. These include some antisolar directions, some directions opposite the orbital angular momentum vector, and a band that crosses the comet orbit plane at an azimuth angle of −40° to the sun direction.
22. R. M. West, *Int. Astron. Union Circ. 6343* (1996).
23. L. Jorda, J. Lecacheux, F. Colas, *Int. Astron. Union Circ. 6344* (1996).
24. W. M. Harris, M. R. Combi, R. K. Honeycutt, B. E. A. Mueller, F. Scherb, *Science* **277**, 676 (1997).
25. Here a_{max} is a simple size distribution cutoff introduced to show the sensitivity of M to maximum grain size. We chose to use this cutoff parameter instead of the maximum liftable grain radius, a_m (*5, 20*), because varying a_m implies varying the grain velocity, whereas here we hold the velocity scaling C at a fixed value determined from the coma spectrum fits. For this comet, a_m is likely to be very large (~10 m).
26. D. Schleicher, *Int. Astron. Union Circ. 6372* (1996); M. J. Mumma, M. A. Di Santi, N. Dello Russo, D. X. Xie, *Int. Astron. Union Circ. 6366* (1996).
27. J. Sarmecanic, M. Fomenkova, B. Jones, *Bull. Am. Astron. Soc.* **28**, 1089 (1996).
28. D. C. Jewitt and H. E. Matthews, *Astron. J.* **113**, 1145 (1997).
29. E. L. Wright, *Astrophys. J.* **346**, L89 (1989); D. C. Jewitt and J. X. Luu, *Icarus* **100**, 187 (1992).
30. J. I. Hage and J. M. Greenberg, *Astrophys. J.* **361**, 251 (1990).
31. In the standard model (*20*) the velocity scaling constant $C = (3C_DC_EV_g\dot{\mu}R/4\rho)^{1/2}$, where C_D is a drag coefficient and C_E corrects for the change in V_g with expansion. To get $V = 40$ m/s for homogeneous spherical grains ($C_D = 2$, $C_E \approx 9/4$) of 0.3 g/cm^3 density and 1-cm radius requires a gas flux of $\dot{\mu} = 4 \times 10^{-4}$ g/cm^2-s for $V_g = 0.29$ km/s (300 K gas). This is higher than the $\dot{\mu} = 5 \times 10^{-5}$ g/cm^2-s that one expects from steady sublimation of a clean ice surface. Making the grains fluffy or fractal can ease the requirement of a high $\dot{\mu}$ because of the lower density ρ and higher drag coefficient C_D [H. U. Keller and W. J. Markiewicz, *Geophys. Res. Lett.* **18**, 249 (1991)]. However, $\dot{\mu}$ could also be higher than the steady sublimation value if the gas release is explosive or jetlike.
32. We thank the AlliedSignal Technical Support Corporation personnel who operate the antennas and support facilities at the Goldstone Deep Space Communications Complex under contract with the Jet Propulsion Laboratory. L.A.M.B. was supported as a research associate of the National Research Council. Part of this research was conducted at the Jet Propulsion Laboratory, California Institute of Technology, under contract with NASA. The remainder of the work was done at the National Astronomy and Ionosphere Center (Arecibo Observatory), which is operated by Cornell University under a cooperative agreement with NSF and with support from NASA.

19 August 1997; accepted 28 October 1997

Spontaneous Formation of Macroscopic Chiral Domains in a Fluid Smectic Phase of Achiral Molecules

Darren R. Link, Giorgio Natale, Renfan Shao,
Joseph E. Maclennan, Noel A. Clark, Eva Körblova,
David M. Walba

A smectic liquid-crystal phase made from achiral molecules with bent cores was found to have fluid layers that exhibit two spontaneous symmetry-breaking instabilities: polar molecular orientational ordering about the layer normal and molecular tilt. These instabilities combine to form a chiral layer structure with a handedness that depends on the sign of the tilt. The bulk states are either antiferroelectric-racemic, with the layer polar direction and handedness alternating in sign from layer to layer, or antiferroelectric-chiral, which is of uniform layer handedness. Both states exhibit an electric field–induced transition from antiferroelectric to ferroelectric.

Chirality has been recognized as an important feature of liquid crystals (LCs) since the time of their discovery (*1*). Now the influence of chirality on phase behavior and macroscopic structure is of major interest in LC science, stimulated in part by the recent discoveries of the blue phases (*2*) and of chiral smectic (Sm) ferroelectric (*3*), antiferroelectric (*4*), and twist grain boundary (*5*) phases. In these and all other known chiral LC phases, the chirality is of molecular origin, being built into the molecular structure upon synthesis, and is essentially permanent. Here we report macroscopically chiral LC phases obtained by the spontaneous chiral organization of achiral molecules. Specifically, we have found coexisting bulk fluid chiral Sm domains of opposite handedness spontaneously formed from molecules that are achiral in the isotropic phase. We provide evidence for the spontaneous formation of chiral layers in a Sm phase made from achiral molecules with bent cores [the homologous compounds **1** (*6*) and **2** (*7*) (Fig. 1)] and provide structural evidence for a symmetry-breaking transition to polar ordering in an achiral LC.

The current interest in the LC behavior of bent-core molecules has been stimulated by the synthetic work of Matsunaga and colleagues (*7, 8*), which includes the design and synthesis of compound **2** and its homologs (*7*). They identified the highest temperature Sm phase in **2** as a smectic C (SmC) and used x-ray layer spacing measurements of the homologous series to argue that the tails are nearly normal to the Sm layers whereas the cores are tilted. They found an 18.5 Å core thickness and, assuming a core conformation giving a 27.5 Å spacing between the alkoxy oxygens of **2**, obtained a core tilt of 48° (*7*). Recently, Watanabe, Takezoe, and co-workers (*6*) synthesized and studied the alkyl homologs of compound **1**, concluding from optical measurements that its highest temperature Sm phase had untilted cores and, from switching current measurements, that there was ferroelectric ordering of the molecular bows, with their arrows pointing in a particular direction that could be switched by an applied electric field. Study by Weissflog *et al.* (*9*) of the octyl homolog of **2** showed an antiferroelectric current response and led them to a model with an untilted core structure and antiferroelectric ordering of the molecular bows. Heppke *et al.* observed ferroelectric switching current dynamics in several other homologs of **1** and **2** (*10*).

Here we present the results of optical microscopy studies of the highest temperature Sm phase of compounds **1** and **2** in the freely suspended film (*11*) and "bookshelf" (*12*) electro-optical geometries. Our work, directed toward revealing the structure of this phase, demonstrates (i) the layer-by-layer antiferroelectric structure of the equilibrium phase, (ii) spontaneous breaking of achiral symmetry in a bulk LC (in this case into chiral Sm layers), (iii) the existence of racemic (R) and homogeneously chiral (H) stacking of these chiral layers, the racemic being the lower free-energy state, (iv) the coexistence of macroscopic, homogeneously chiral domains of opposite handedness, which maintain their handedness during electro-optic switching and are identifiable by their chiral response to applied electric field, and (v) "sergeants-and-soldiers" biasing of the global chirality by addition of chiral dopant. On the basis of these observations, we have adopted the nomenclature "SmCP$_A$" for this phase (*13*). The SmCP$_A$ phase of both compounds **1** and **2** behaved in essentially identical fashion in the film and

---

D. R. Link, G. Natale, R. Shao, J. E. Maclennan, N. A. Clark, Department of Physics, Condensed Matter Laboratory, University of Colorado, Boulder, CO 80309, USA. E. Körblova and D. M. Walba, Department of Chemistry and Biochemistry, University of Colorado, Boulder, CO 80309, USA.

bookshelf cell studies.

We recently reported using freely suspended films, drawn in air with an integer number of Sm layers and imaged with depolarized reflected light microscopy (DRLM) (*14*) using oblique laser illumination, to probe electric dipole density in tilted Sm phases (*15*). Conventional antiferroelectric (SmC$_\mathrm{A}$*) phases (*4*) exhibit a dramatic even-odd effect versus layer number: Films of an even number of layers have polarization only in the molecular tilt plane, whereas films of an odd number of layers of chiral materials have polarization only normal to the tilt plane (*15*). Here we apply the DRLM technique to probe the ground-state structure of the SmCP$_\mathrm{A}$ phase. Films of uniform thickness with the layer number *N* ranging from 2 to 10, as well as films with layer steps, were prepared for study by drawing them in the SmCP$_\mathrm{A}$ phase over a 5-mm-diameter hole in a glass cover slip. Film thickness was determined by laser reflectivity (*11*). In both compounds **1** and **2**, the SmCP$_\mathrm{A}$ phase was stabilized relative to the lower temperature S2 phase, with, for example, the SmCP$_\mathrm{A}$ phase found at temperatures $138°\mathrm{C} < T < 160°\mathrm{C}$ in two-layer films of compound **1**, for which the range of the SmCP$_\mathrm{A}$ phase in the bulk is only ~5°C.

Our DRLM observations with oblique incidence and slightly uncrossed polarizers showed that an optic axis in the SmCP$_\mathrm{A}$ phase is tilted relative to the layer normal and revealed the smooth brush patterns characteristic of films of tilted Sm phases (*14*–*16*). We refer to the plane containing this tilted optic axis as the tilt plane (Fig. 1) and give its orientation in the layer plane by the unit vector director **c**. Ferroelectricity in films can be detected easily by applying a small electric field ($E \sim 10$ V/cm) in the plane of the film. If the film is ferroelectric, the field will couple linearly to the ferroelectric dipoles, rotating them so that they orient along the field (*14*). When a weak electric field was applied to films in the SmCP$_\mathrm{A}$ phase, we observed a striking odd-even effect (Fig. 2): Odd-*N* regions were ferroelectric with **c** oriented normal to the electric field, which would require chirality and is typical of tilted chiral (ferroelectric) Sm phases; however, even-*N* regions did not react to the field and were thus not ferroelectric. Therefore, the ground state of the SmCP$_\mathrm{A}$ phase is in fact antiferroelectric, with $\mathbf{P}_\mathrm{b}$, the layer polarization in the plane normal to **c**, alternating from layer to layer. Additionally, the refractive index for optical polarization along **c** was smaller than that for optical polarization normal to **c**, a condition not found in typical Sm phases that indicates a strong biaxiality and ordering of molecular planes normal to **c**. These results lead us to propose the layer structure indicated in Fig. 1, which has ferroelectric polar ordering of the molecular bows characterized by the arrow direction **b**, oriented parallel to the polar plane (as would the arrow in a bow-arrow combination), and a resulting polarization $\mathbf{P}_\mathrm{b}$ locally normal to the molecular tilt direction **c**. By varying *E*, we uniquely mapped with DRLM the spatial variation of the **b**-**c** couple over the film surface (*16*), revealing domains of opposite chirality separated by sharp domain boundaries in SmCP$_\mathrm{A}$-phase films of uniform thickness (Fig. 3A). The jump in brush intensity as the domain wall was crossed indicates that the orientation of **c** changed by π upon crossing the boundary. Although this experiment was not sensitive to the sign of **b**, **b** can be mapped unambiguously with an applied *E* field. In Fig. 3, B and C, for example, the field-induced orientation of **b** seems to be uniform except for the 2π reorientations of

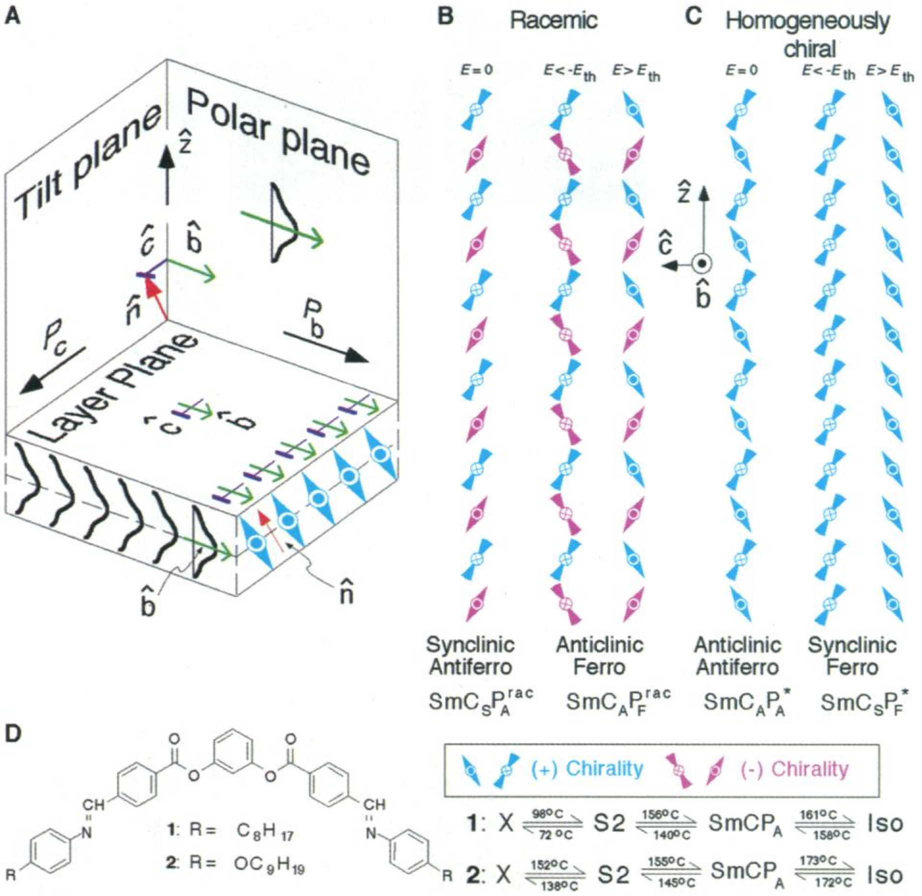

Fig. 1. (**A**) Geometry of the SmCP$_\mathrm{A}$ phase, showing the layer, tilt, and polar planes, the result of three distinct symmetry-breaking events: the formation of fluid Sm layers normal to **z**, the tilt of the molecular bows in the direction given by **c**, and the polar ordering of the molecular bows along the "arrow" **b**. (**B** and **C**) Layer organization in the SmCP$_\mathrm{A}$ phase showing the antiferroelectric racemic and homogeneously chiral states at zero applied electric field ($E = 0$) and the corresponding ferroelectric states for fields beyond the threshold E_th. (**D**) Compounds **1** (*6*) and **2** (*7*) and their phase diagrams.

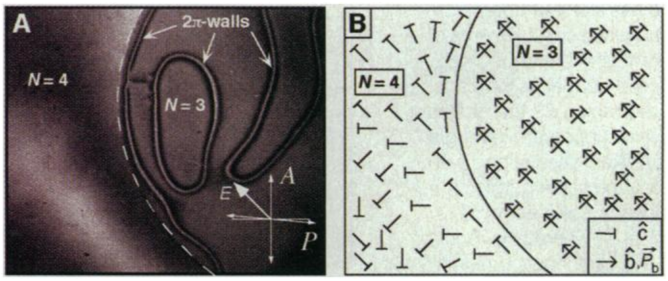

Fig. 2. (**A**) DRLM microphotograph with normally incident illumination showing the electric-field response of three- and four-layer-thick films of compound **1** in the SmC$_\mathrm{S}$P$_\mathrm{A}$ phase. Indicated are the incident (*P*) and reflected (*A*) optical polarizations, applied electric field **E**, and the layer step-edge location (dashed line). Using this optical arrangement, (**B**) a sketch of the orientation of **b** can be drawn, showing that in the $N = 3$ region, **b** is oriented by the field, trapping 2π walls (2π rotations of the **b**-**c** couple), indicating a ferroelectric response. The $N = 4$ region is antiferroelectric, as its smoothly varying $E = 0$ director structure is unaffected by the field.

b-**c**, which show up as "2π walls" that are away from the domain boundaries. Note that **b** must be continuous across the domain boundaries: If it were not, then the *E* field would trap a π wall at every domain boundary, which is not seen. The light-intensity dependence (Fig. 3A) shows that it is the orientation of **c** that changes sign at the domain boundaries. Antiferroelectricity implies that **b** (and hence $\mathbf{P}_b$) have opposing orientations in adjacent layers, but the observation of optic axis tilt even in $N = 2$ films implies the same tilt direction **c** in all layers of a particular tilt domain, that is, structures that are "synclinic" with respect to the tilt. This synclinic tilt in **c** with antiferroelectricity in **b** indicates that alternating layers have chiral conformations of opposite handedness, in contrast to tilted chiral ferroelectrics (SmC*, synclinic tilt and the same handedness in every layer) and antiferroelectrics [SmC_A*, anticlinic tilt and the same handedness in every layer (*4*)]. Analysis of the tilt plane ($\mathbf{p}_c$) and polar plane ($\mathbf{p}_b$) polarization densities in $N = 2$ and 3 films (Fig. 3, D and E) provides further evidence for a synclinic tilt in **c** with antiferroelectricity in **b**. Specifically, an $N = 2$ structure that is anticlinic in **c** would have $\mathbf{P}_c = \int \mathbf{p}_c dz \neq 0$, which, from our earlier SmC_A* experiments (*15*), would be easily observable, that is, $N = 2$ films would be ferroelectric along **c**, but this is not the case. Only $\mathbf{P}_b$ is nonzero, and then only in odd-*N* films. From these observations on the SmCP_A phase, we conclude that the film structure is $\text{SmC}_S\text{P}_A{}^{\text{rac}}$ (*13*), a spontaneous symmetry breaking to a synclinic antiferroelectric, and therefore racemic, stacking of chiral layers. Such structures have been found in crystals of achiral molecules (*17*), but have not been previously reported in LCs.

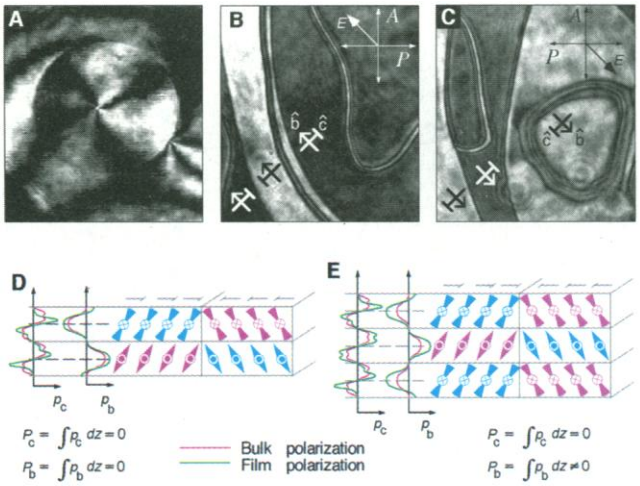

Fig. 3. (**A**) A two-layer film ($N = 2$) of compound **1** in the SmC_SP_A phase with a circular domain wall separating two domains of opposite tilt direction and chirality. (**B**) A three-layer film ($N = 3$) with several tilt-switching domains, viewed through crossed polarizers oriented at 45° to a 10 V/cm applied electric field. This configuration with oblique incidence generates optical contrast with the change in tilt at the domain boundaries. The multiline defects are 2π walls (2π rotations of **b**-**c**) trapped by the field. The absence of π walls at the domain boundaries indicates that **b** is continuous across the boundaries. (**C**) Field-reversed state of (B). (**D** and **E**) Schematic structure of $N = 2$ and 3 films, respectively, showing the synclinic tilt in **c**, antiferroelectricity in **b**, and possible corresponding polarization densities $\mathbf{p}_c$ and $\mathbf{p}_b$, each density having the appropriate symmetry. With the synclinic tilt structure (**c** having the same sign in adjacent layers), $\mathbf{P}_c$, the net polarization along **c**, is zero for any *N*, and $\mathbf{P}_b$, the net polarization along **b**, is nonzero for odd-*N* films, as is observed. This synclinic tilt in **c** with antiferroelectricity in **b** means that alternating layers have chiral conformations of opposite handedness, as indicated by the blue-magenta color coding.

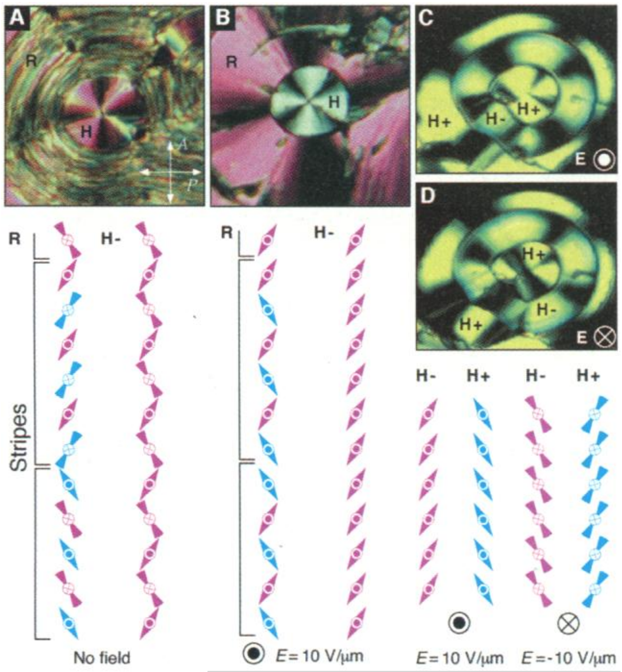

Fig. 4. Transmission polarized light micrographs of the SmCP_A phase of compound **2** in a focal conic planar aligned (bookshelf) cell between crossed polarizer (*P*) and analyzer (*A*), and corresponding schematic organization of the layers in the phase. (**A**) Focal conic area with $E = 0$ showing an R region with distinct stripes running parallel to the Sm layers, and an H region, which appears SmA-like and has a uniform purple birefringence color. (**B**) Area of (A) with $E = 10$ V/μm $> E_{\text{th}}$, applied normal to the page. In the region R, the stripes have disappeared, leaving a SmA-like orientation with nearly the same purple birefringence color as region H at $E = 0$, whereas in region H, the birefringence has increased in the applied field, and the extinction brushes have rotated to a SmC* state. (**C** and **D**) Division of H into subregions H+ and H−, having opposite signs of $\mathbf{P}_b$ and in which extinction brushes consequently rotate in opposite directions. These domains maintain their handedness even under conditions of repeated field reversal with $E > E_{\text{th}}$ (D).

In order to further probe the structure of the SmCP_A phase, compounds **1** and **2** were used to fill 4-μm-thick transparent capacitor electro-optic cells made from indium-tin oxide coated glass in the SmCP_A phase, and were subjected to a field **E** while being viewed in transmission through the crossed polarizers of an optical microscope. The SmCP_A phase of both materials adopted a random focal conic texture with the Sm layers essentially normal to the glass plates (planar alignment) (Fig. 4). Two types of regions were visible: region R, which has distinct stripes running parallel to the Sm layers and typically occupies the majority of the sample, and region H, which appears SmA-like (that is, smoothly birefringent, with an orientation of the extinction brushes characteristic of the SmA phase, and a uniform birefringence color, in this case pink). Regions R and H behave quite differently upon application of an *E* field above a threshold voltage ($E_{\text{th}} \sim 5$ V/μm). For a given sign of *E*, the stripes in region R disappear, leaving a smoothly birefringent SmA orientation of the extinction brushes and nearly the same pink birefringence color as in region H when no field is applied. This brush orientation is similar to that found by Takezoe and colleagues (*6*): The extinction brushes do not rotate when the sign of the applied field is reversed, remaining SmA-like for *E* both above and below E_{th}. However, an above-threshold field produces in region H two concurrent changes: The birefringence increases with increasing *E*, generating in this case a yellow birefringence color, and the extinction brushes rotate as they would in a chiral ferroelectric Sm phase, for example, clockwise for one sign of field and counterclockwise for the other (Fig. 4B). Region H itself is divided into two distinct subregions, H+ and H−, which have different handedness and therefore differ in the sign of P_b ($P_b > 0$ if $\mathbf{P}_b$ is parallel to $\mathbf{b} = \mathbf{z} \times \mathbf{c}$). Upon application of a given sign of electric field, the H+ and H− extinction brushes rotate in opposite directions (Fig. 4C). Regions H+ and H− can coexist within the same Sm focal conic domain. Generally, such domains are stable in the presence of applied field, that is, the field does not alter the layer chirality. An exception is found in compound **2**, wherein, if the SmCP$_A$ phase is obtained by heating from the lower temperature "blue" phase, the H states are initially the majority, often occupying the entire area. Application of a square-wave switching field induces a chiral SmC-like brush rotation, with each local area maintaining its sign of polarization. However, this switching promotes their conversion to R, particularly at higher temperatures in the phase.

Figure 4 illustrates the structures we propose for the field-on and field-off states of the R and H regions. The H regions are chiral, antiferroelectric in **b**, and anticlinic in **c**, and thus, with $E = 0$, are SmC$_A$P$_A$*, similar in structure to the SmC$_A$* phase. The resulting state is biaxial and, with an optic axis along the layer normal, appears SmA-like. One would expect a helixing of the **b**-**c** couple with travel along $\mathbf{z}$ in a bulk H sample, but this is not observed in our thin surface-stabilized cells. The increase in birefringence in the H regions upon field application is a result of the progressive loss of the strict tilt alternation at $E = 0$ to form uniformly tilted chiral domains. These domains are ferroelectric SmC*-like, except that domains with either sign of P_b (in both cases with $\mathbf{P}_b$ along $\mathbf{E}$ but of opposite tilt) coexist in the sample. The racemic state with $E > E_{th}$, denoted SmC$_A$P$_F^{rac}$ (*13*), is also anticlinic in **c** (and thus also appears SmA-like) and is observed to have nearly the same birefringence as the H state with $E = 0$, consistent with this model. Removal of the field from the racemic state produces an interesting relaxation process to the antiferroelectric SmC$_S$P$_A^{rac}$ ground state. As E is reduced, the molecules in one subset of layers, either the even or the odd, must rotate to give antiferroelectricity in **b** (Fig. 4B). If the odd-layer molecules rotate, then a domain (stripe) of one sign of tilt is obtained at $E = 0$, whereas if the even-layer molecules rotate, a stripe of the other sign of tilt forms. This process leads to the formation of domains of energetically degenerate states of opposite tilt (one obtainable from the other by a π rotation of **b**-**c** about $\mathbf{z}$) and to the distinctive stripe pattern of the R regions at $E = 0$. Note that because the R state is racemic, there is no tendency for **c** to twist, and therefore, there is no helix (in the $N = 2$ film, the polar plane polarizations $\mathbf{P}_b$ of the two layers are exactly opposed in equilibrium).

The observation that the minority H states are close in free energy to the equilibrium R state suggested the possibility that addition of chiral dopant could modify the relative free energies of the R and H states and make the H state the more stable. In mixtures of as little as 1 weight % of the SmC* material W314 (*18*) with compound **2**, the H state is markedly stabilized, converting the majority of the cell area to the H state with negative P_b (the same polarization sign as W314), while maintaining the antiferroelectric $E = 0$ state. This is a bulk LC analog of the "sergeants and soldiers" chiralization of the achiral polyisocyanate polymer recently reported by Green and co-workers (*19*). In dilute solution, these polymer molecules exhibit a spontaneous symmetry breaking to a chiral state, forming helical rodlike structures. Changing a few percent of the side groups to be chiral "sergeants" causes all of the achiral side group "soldiers" to twist with a single handedness. Precisely the same effect is observed in our experiments in a bulk LC phase, where the low concentration of chiral dopant is sufficient to bias the chirality to a single handedness. This behavior may be describable by a theoretical model analogous to that developed for the polyisocyanates (*20*).

Both the free film and electro-optic cell experiments show that the SmCP$_A$ phase is a smectic of liquidlike layers. The SmCP$_A$ films exhibit the low-viscosity in-plane flow and dramatic orientation fluctuations of **c** characteristic of SmC films, and the SmCP$_A$ electro-optic response speed in the cells (400 μs at 8 V/μm) is also comparable to typical SmC values. Also, near the point of SmCP$_A$–isotropic phase coexistence, the shapes of Sm focal conic domains surrounded by isotropic phase are quite dynamic, readily changing in response to applied fields. Thus, the achiral symmetry breaking described is achieved in a fluid Sm phase.

The appearance of the SmCP$_A$ phase in films with only two or three layers indicates that the basic collective effects generating the structure are intralayer, as is the case for the symmetry-breaking molecular tilt in the SmC (*11*) and SmC$_A$* (*21*) phases of typical rod-shaped molecules. For the known SmC phases of achiral rod-shaped molecules, the mirror symmetry about the tilt plane is maintained, whereas for the bow-shaped molecules studied here, there is an additional intralayer collective polar ordering of the arrow directions along **b** that eliminates this mirror symmetry. This polar ordering is related to the distinctive bent-core shape of the molecules but is probably not strongly related to, or affected by, the molecular tilt. Thus, the chirality of the SmCP$_A$ phase arises from the peculiar geometrical relation within the Sm phase of two essentially independent, strongly stabilized broken symmetries: intralayer collective polar ordering of the molecular bows and intralayer collective tilt of the molecular planes. The stabilization of the relative chirality and orientation of adjacent layers is an energetically secondary effect that may be altered by relatively weak applied fields or by chiral doping.

REFERENCES AND NOTES

1. The discovery of LCs is generally taken to be the observation of the chiral nematic phase in optically active cholesteryl benzoate by F. Reinitzer [*Monatsh. Chem.* **9**, 421 (1888)].
2. D. Armitage and F. P. Price, *J. Phys (Paris)* **36** (colloque C-1), C1-133 (1975); S. A. Brazovskii, *Zh. Eksp. Teor. Fiz.* **68**, 175 (1975) [*Sov. Phys. JETP* **41**, 85 (1975)].
3. R. B. Meyer, L. Liebert, L. Strzelecki, P. Keller, *J. Phys. (Paris)* **36**, L69 (1975).
4. A. Fukuda, Y. Takanashi, T. Isozaki, K. Ishikawa, H. Takezoe, *J. Mater. Chem.* **4**, 997 (1994).
5. S. R. Renn and T. C. Lubensky, *Phys. Rev. A* **38**, 2132 (1988); J. W. Goodby *et al.*, *Nature* **337**, 449 (1989).
6. T. Niori, T. Sekine, J. Watanabe, T. Furukawa, H. Takezoe, *J. Mater. Chem.* **6**, 1231 (1996).
7. T. Akutagawa, Y. Matsunaga, K. Yasuhara, *Liq. Cryst.* **17**, 659 (1994).
8. Y. Matsunaga and S Miyamoto, *Mol. Cryst. Liq. Cryst.* **237**, 311 (1993); H. Matsuzaki and Y. Matsunaga, *Liq. Cryst.* **14**, 105 (1993).
9. W. Weissflog *et al.*, in *Abstracts, European Conference on Liquid Crystals, Zakopane, Poland*, ISBN 83-911181-8-1 (1997), p. 201; W. Weissflog, private communication.
10. G. Heppke *et al.*, in *Abstracts, European Conference on Liquid Crystals, Zakopane, Poland*, ISBN 83-911181-8-1 (1997), p. 34.
11. C. Y. Young, R. Pindak, N. A. Clark, R. B. Meyer, *Phys. Rev. Lett.* **40**, 773 (1978).
12. N. A. Clark and S. T. Lagerwall, *Appl. Phys. Lett.* **36**, 899 (1980).
13. The notation SmCP derives from the key broken symmetries of this phase: Sm (for Sm layering), C (the usual notation for molecular tilt), and P (for polar ordering). Optional subscripts describe the relative organization of adjacent layers: C$_A$, anticlinic tilt; C$_S$, synclinic tilt; P$_A$, antiferroelectric polar order; and P$_F$, ferroelectric polar order. Thus, the field-free phase observed is SmCP$_A$, with the racemic ground state R being SmC$_S$P$_A^{rac}$ and the homogeneously chiral state H being SmC$_A$P$_A$* (the usual * to indicate chirality). The corresponding field-induced ferroelectric states are SmC$_A$P$_F^{rac}$ and SmC$_S$P$_F$*, respectively. These four SmCP substates are illustrated in Fig. 1. Molecules like those studied here have been called "banana-shaped" (*6, 9, 10*). We prefer to use "bow-shaped" because in a drawn bow, the bow effectively represents the molecule, and the arrow, the direction of polar ordering.
14. R. Pindak, C. Y. Young, R. B. Meyer, N. A. Clark, *Phys. Rev. Lett.* **45**, 1193 (1980).
15. D. R. Link, J. E. Maclennan, N. A. Clark, *ibid.* **77**, 2237 (1996).
16. J. Z. Pang, C. D. Muzny, N. A. Clark, *ibid.* **69**, 2783 (1992).
17. For a recent example, see M. E. Brown, J. D. Chaney, B. D. Santasiero, M. D. Hollingsworth, *Chem. Mater.* **8**, 1588 (1996).
18. D. M. Walba *et al.*, *Ferroelectrics* **121**, 247 (1991).
19. M. M. Green *et al.*, *Science* **268**, 1860 (1995); S. Lifson, C. Andreola, N. C. Peterson, M. M. Green, *J. Am. Chem. Soc.* **111**, 8850 (1989).
20. J. V. Selinger and R. L. B. Selinger, *Phys. Rev. Lett.* **76**, 58 (1996).
21. D. Fliegner and C. Bahr, *ibid.* **70**, 1842 (1993).
22. This work was supported by NASA grant NAG3-1846, NSF grant DMR-96-14061, and NSF Materials Research Group grant 92-24168.

14 July 1997; accepted 20 October 1997